

Significantly enhanced photocatalytic hydrogen evolution under visible light over CdS embedded on metal–organic frameworks†

Cite this: DOI: 10.1039/c3cc43218a

Received 1st May 2013,
Accepted 11th June 2013

DOI: 10.1039/c3cc43218a

www.rsc.org/chemcomm

Jiao He, Zhiying Yan, Jiaqiang Wang,* Jiao Xie, Liang Jiang, Yangmei Shi, Fagui Yuan, Fei Yu and Yuejuan Sun

We demonstrated that embedding of CdS on MOFs could significantly increase the photocatalytic efficiency of CdS for visible light-driven hydrogen production.

In view of increasingly serious energy and environmental problems, considerable efforts have been invested in photocatalytic hydrogen production from water splitting.¹ Chalcogenide nanomaterials are attractive because they have ideal edge positions of the valence and conduction bands for the reduction of water molecules utilizing the abundant visible region of sunlight.^{1b–d} Many approaches to improving the hydrogen production rate and photostability of pure CdS particles have been investigated. For example, CdS loaded with MoS₂,² co-loaded with Pt and PdS,³ incorporation of CdS particles into the mesopores of Ti-MCM-41⁴ and introduction of graphene nanosheets into CdS⁵ have been used.

On the other hand, metal–organic frameworks (MOFs) have gained widespread attention recently due to their high surface areas, crystalline open structures, tunable pore size, and functionality. They also have a high volume fraction of active metal sites. These properties have inspired many potential applications in catalysis.⁶ Because of the well-defined crystal structures of MOFs and controllable chromophore distances *via* crystal engineering, highly crystalline MOFs have provided an ideal platform for designing molecular solids for light harvesting.⁷ Indeed, UiO-67,⁸ UiO-66,⁹ Pt@UiO MOFs,^{7c} amino-functionalized Ti(IV) MOFs,¹⁰ Ru-based MOFs,¹¹ Zn-MOFs¹² and Zn₄O-based MOFs¹³ show intrinsic photoactivities. However they are not as effective as semiconductor catalysts.¹⁴ Compared with MOFs, the semiconductor@MOF heterostructures show great advantages due to their synergistic effect. Particularly, ZnO@ZIF-8¹⁵ and TiO₂@MOF-5¹⁶ exhibited distinct optical properties. ZnO@MOF-5¹⁷ has also been synthesized. However, the photocatalytic activities of these heterostructures, in

particular, chalcogenide nanoparticles embedded in MOFs, to our knowledge have not been thoroughly investigated.

Herein, we report for the first time the fabrication of CdS embedded MIL-101 (Cr₃F(H₂O)₂O[BDC]₃·*n*H₂O, BDC = terephthalic acid). We chose this because this Cr MOF shows good resistance to air, water, common solvents, and thermal treatment.^{6d} MIL-101 did not exhibit any photocatalytic activity by itself. However, it is demonstrated in this research that the photocatalytic activity of CdS embedded on MIL-101 for hydrogen evolution under visible-light is significantly enhanced in comparison with bare CdS when using Pt as a co-catalyst.

MIL-101 was synthesized first and then CdS nanoparticles were embedded on it at 0, 5, 10, 20 and 50% CdS by weight, herein labelled as CdS/MIL-101(*X*) where *X* = 5, 10, 20 and 50%. X-ray diffraction (XRD) measurements (ESI,† Fig. S1) proved that MIL-101 was successfully synthesized and its structure was not changed after modification.^{6d,18} The embedded CdS was confirmed to be cubic crystalline (JCPDS 80-0019)⁵ with the average crystallite sizes of between 2 to 3 nm calculated using the Scherrer formula for the (111) facet diffraction peak.

The N₂ adsorption–desorption isotherm (ESI,† Fig. S2) of MIL-101 is of type I indicating the presence of two kinds of micropores as described in the literature.^{18a} A type II isotherm is observed on pure CdS indicating nonporous or macroporous structure.⁵ When CdS was introduced into MIL-101, type I adsorption–desorption isotherms were observed but the uptake at *P/P*₀ around 0.1 and 0.2 damped with increasing amounts of CdS. The Brunauer–Emmett–Teller (BET) surface area (*S*_{BET}) and the pore volume of MIL-101 decrease with the increasing CdS content (Table 1). This is attributed to pore blockage. Nevertheless, CdS/MIL-101 maintained its porous structure and high specific surface area.

The morphologies of the samples were further analyzed using a transmission electron microscope (TEM). It is seen that CdS aggregates can be formed on the external surface of MIL-101 octahedral crystals (Fig. 1). High-resolution TEM reveals a lattice spacing of 0.33 nm corresponding to the interplanar distance between adjacent (111) crystallographic planes of cubic CdS.

Fig. 2a shows a comparison of the UV-vis absorbance spectra of the samples. The significant absorption of pure CdS at

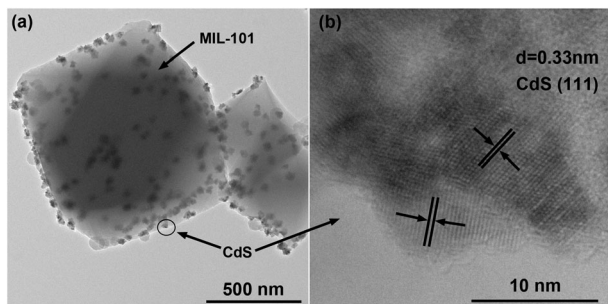
The Universities' Center for Photocatalytic Treatment of Pollutants in Yunnan Province, School of Chemical Sciences & Technology, Yunnan University, Kunming 650091, P. R. China. E-mail: jqwang@ynu.edu.cn; Fax: +86 871 65031567; Tel: +86 871 65031567

† Electronic supplementary information (ESI) available: Synthetic procedures, characterization and methods of photocatalytic hydrogen production. See DOI: 10.1039/c3cc43218a

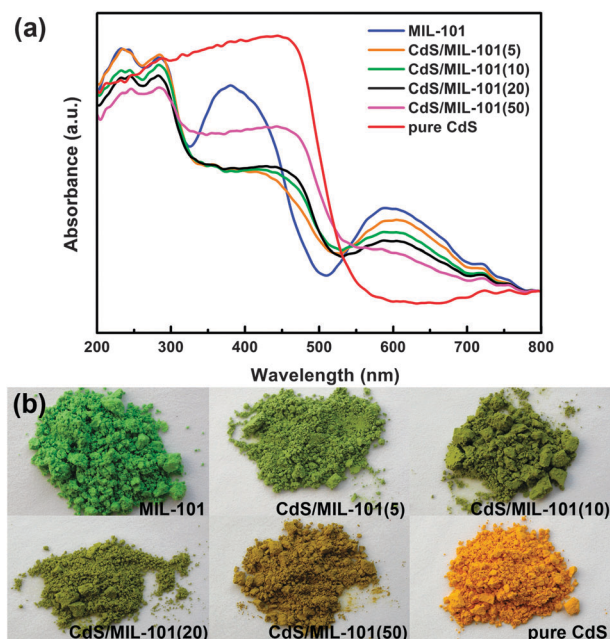
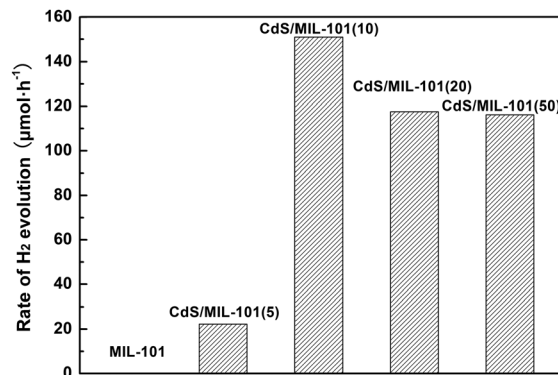
Table 1 Summary of textural properties and activities for photocatalytic H₂ production of the samples

Samples	S_{BET} ($\text{m}^2 \text{g}^{-1}$)	Pore volume ($\text{cm}^3 \text{g}^{-1}$)	Pore size (nm)	Activity ($\text{mmol g}_{\text{CdS}}^{-1} \text{h}^{-1}$)
MIL-101	2909.85	1.34	3.3	—
CdS/MIL-101(5)	2449.12	1.13	3.9	22.2
CdS/MIL-101(10)	2340.33	1.07	3.5	75.5
CdS/MIL-101(20)	1913.11	0.89	4.3	31.5
CdS/MIL-101(50)	1167.32	0.56	4.8	11.6
CdS	131.83	0.12	6.0	33.8
CdS mixed MIL-101 ^a	—	—	—	14.1

^a The weight ratio of CdS is 10 wt%, the same as CdS/MIL-101(10).

**Fig. 1** (a) The TEM image of CdS/MIL-101(10) and (b) the HRTEM image of embedded CdS aggregates.

wavelengths shorter than 500 nm can be attributed to the intrinsic bandgap absorption of cubic CdS. The band positions of MIL-101 in the UV region can be assigned to $\pi-\pi^*$ transitions of ligands¹⁹ and the bands in the visible region belong to the d-d spin-allowed transition of the Cr^{3+} (d^5).²⁰ The intensity of the two bands of MIL-101 in the UV and visible range decreased

**Fig. 2** (a) UV-vis diffuse reflectance spectra and (b) photographs of pure MIL-101, CdS/MIL-101(*X*) (*X* = 5, 10, 20, 50%) and pure CdS.**Fig. 3** H₂ production over MIL-101 embedded with different amounts of CdS under visible light (20 mg of the catalyst, 0.5 wt% Pt loaded).

after incorporation of CdS. Furthermore, the absorption edges of the CdS embedded MIL-101 showed clear red-shifts towards the absorption edge of pure CdS. Fig. 2b shows the corresponding photos of all the samples, indicating that their colors change from green to yellow with increasing amounts of CdS.

The CdS/MIL-101 assemblies were photodeposited with Pt particles to obtain Pt@CdS/MIL-101 and then examined for their photocatalytic activities for hydrogen evolution in lactic acid aqueous solution²¹ under visible-light ($\lambda > 420 \text{ nm}$) irradiation.²² As shown in Fig. 3, no appreciable H₂ evolution was detected over MIL-101 in the absence of CdS. This indicates that MIL-101 did not act as an effective semiconductor photocatalyst by itself. The TEM images of Pt@CdS/MIL-101 (ESI,† Fig. S3) show many small Pt nanoparticles deposited on the CdS surface but not on MIL-101 after *in situ* photoreduction. After embedding only 5 wt% of CdS on MIL-101, the rate of H₂ evolution increased to 22 $\mu\text{mol h}^{-1}$ (Fig. 3). The maximum H₂ evolution was found at 10 wt% (10% w/w) CdS. In the presence of the same amount of CdS (2 mg), the H₂ production rate increased in the following order: CdS mixed MIL-101 < bare CdS < CdS/MIL-101(10) (Table 1). The photostability of CdS/MIL-101(10) was investigated over four consecutive runs of totally 5 h. The long-term durability of the catalysts was also satisfactory (ESI,† Fig. S4). The XRD patterns of the fresh and used CdS/MIL-101(10) were almost similar implying that CdS/MIL-101(10) is stable during the photocatalytic reaction (ESI,† Fig. S5).

The success in enhancement of the photocatalytic H₂ production activity by using CdS/MIL-101 encouraged us to extend this approach to other MOFs or mesoporous materials. MOF-5, the most-studied MOF with respect to its activity as a semiconductor,²³ and MCM-41 were selected. Although the experimental evidence supporting the behavior of MOF-5 as a semiconductor has been provided,^{23a,24} different from MIL-101, CdS modified MOF-5 exhibited negligible activity for the photocatalytic hydrogen evolution under our experimental conditions. The H₂ production observed increased in the following order: CdS embedded on MCM-41 < bare CdS < CdS embedded on MOF-5 < CdS/MIL-101 (ESI,† Fig. S6). On top of this, MOF-5 is not stable when exposed to air, water and thermal treatment. So the activity of CdS embedded on MOF-5 is not so effective. This is probably due to the collapse of the framework after CdS incorporation (ESI,† Table S1). In comparison with MIL-101 and MOF-5, MCM-41 showed decreased H₂ production although it

possesses a mesoporous structure with a considerable specific surface area. This highlights the significance of MOF based materials.

On the basis of the mechanistic aspects described above, we tentatively propose the following mechanism: irradiated light is absorbed partly by the MIL-101 photosensitizer unit (because of the absorbance differences) and mainly by CdS. The redox potential ($\text{Cr}^{3+}/\text{Cr}^{2+}$) of MIL-101 was +0.49 V vs. NHE (normal hydrogen electrode),²⁵ and the reduction potential of the excited photosensitizer unit was calculated to be -1.57 V vs. NHE.²⁶ And the CdS valence and conduction band edges have been reported as +1.88 and -0.52 V, respectively, vs. NHE.²⁷ After the absorption of visible light by MIL-101(Cr^{III}), an excited state of MIL-101($\text{Cr}^{\text{III}*}$) is formed. Electrons are then transferred from MIL-101($\text{Cr}^{\text{III}*}$) to the conduction band of CdS and then to the loaded Pt particles where the protons are reduced to form molecular H_2 . At the same time, the reduced state MIL-101(Cr) species return to the ground state, accomplishing a complete water reduction reaction. Additionally, the CdS can also be excited by absorbing photons of light having energy exceeding its band gap and then transferring electrons directly to the Pt to produce H_2 .

The enhancement of the photocatalytic activity of CdS after MOF hybridization can be attributed to the fact that MIL-101 has a large specific surface area which allows effective dispersion of embedded CdS particles. This provides more active adsorption sites and photocatalytic reaction centers which favor enhanced photocatalytic activity. Moreover, the sensitization of CdS by MIL-101 is effective and superior to bare CdS, which makes it a photocatalyst with good visible light harvesting capability.

In summary, we have demonstrated for the first time that the embedding of CdS on MOFs significantly increases the photocatalytic efficiency of CdS. In the context of their application to visible-light-promoted photocatalytic hydrogen production, MOFs possess great flexibility in terms of framework design because the choice of selecting the suitable host MOF depending on the linker (organic molecules), the connector (metal atoms) or the both²⁸ can be widely varied.

This work was supported by the National Natural Science Foundation of China (NSFC-YN 21063016, U1033603) and the Program for Innovative Research Teams (in Science and Technology) at the University of Yunnan Province.

Notes and references

- (a) K. Maeda, K. Teramura, D. Lu, T. Takata, N. Saito, Y. Inoue and K. Domen, *Nature*, 2006, **440**, 295; (b) F. E. Osterloh, *Chem. Mater.*, 2007, **20**, 35–54; (c) A. Kudo and Y. Miseki, *Chem. Soc. Rev.*, 2009, **38**, 253–278; (d) R. Abe, *J. Photochem. Photobiol. C*, 2010, **11**, 179–209; (e) X. Chen, S. Shen, L. Guo and S. S. Mao, *Chem. Rev.*, 2010, **110**, 6503; (f) A. Kubacka, M. Fernandez-Garcia and G. Colon, *Chem. Rev.*, 2012, **112**, 1555–1614.
- X. Zong, H. Yan, G. Wu, G. Ma, F. Wen, L. Wang and C. Li, *J. Am. Chem. Soc.*, 2008, **130**, 7176–7177.
- H. Yan, J. Yang, G. Ma, G. Wu, X. Zong, Z. Lei, J. Shi and C. Li, *J. Catal.*, 2009, **266**, 165–168.
- S. Shen and L. Guo, *Mater. Res. Bull.*, 2008, **43**, 437–446.
- Q. Li, B. Guo, J. Yu, J. Ran, B. Zhang, H. Yan and J. R. Gong, *J. Am. Chem. Soc.*, 2011, **133**, 10878–10884.
- (a) J. M. Roberts, B. M. Fini, A. A. Sarjeant, O. K. Farha, J. T. Hupp and K. A. Scheidt, *J. Am. Chem. Soc.*, 2012, **134**, 3334–3337; (b) D. Farrusseng, S. Aguado and C. Pinel, *Angew. Chem., Int. Ed.*, 2009, **48**, 7502–7513; (c) M. Ranocchiari and J. A. van Bokhoven, *Phys. Chem. Chem. Phys.*, 2011, **13**, 6388–6396; (d) N. V. Maksimchuk, K. A. Kovalenko, V. P. Fedin and O. A. Kholdeeva, *Adv. Synth. Catal.*, 2010, **352**, 2943–2948; (e) A. Dhakshinamoorthy, M. Alvaro and H. Garcia, *Chem. Commun.*, 2012, **48**, 11275–11288; (f) A. Dhakshinamoorthy and H. Garcia, *Chem. Soc. Rev.*, 2012, **41**, 5262–5284.
- (a) C. G. Silva, A. Corma and H. Garcia, *J. Mater. Chem.*, 2010, **20**, 3141; (b) C. H. Hendon, D. Tiana and A. Walsh, *Phys. Chem. Chem. Phys.*, 2012, **14**, 13120–13132; (c) J.-L. Wang, C. Wang and W. Lin, *ACS Catal.*, 2012, **2**, 2630–2640.
- C. Wang, Z. Xie, K. E. deKrafft and W. Lin, *J. Am. Chem. Soc.*, 2011, **133**, 13445–13454.
- C. Gomes Silva, I. Luz, F. X. Llabres i Xamena, A. Corma and H. Garcia, *Chem.–Eur. J.*, 2010, **16**, 11133–11138.
- Y. Fu, D. Sun, Y. Chen, R. Huang, Z. Ding, X. Fu and Z. Li, *Angew. Chem., Int. Ed.*, 2012, **51**, 3364–3367.
- Y. Kataoka, Y. Miyazaki, K. Sato, T. Saito, Y. Nakanishi, Y. Kiatagawa, T. Kawakami, M. Okumura, K. Yamaguchi and W. Mori, *Supramol. Chem.*, 2011, **23**, 287–296.
- J. Gascon, M. D. Hernandez-Alonso, A. R. Almeida, G. P. van Klink, F. Kapteijn and G. Mul, *ChemSusChem*, 2008, **1**, 981–983.
- H. Khajavi, J. Gascon, J. M. Schins, L. D. A. Siebbeles and F. Kapteijn, *J. Phys. Chem. C*, 2011, **115**, 12487–12493.
- Y. Miyazaki, Y. Kataoka and W. Mori, *J. Nanosci. Nanotechnol.*, 2012, **12**, 439–445.
- W. W. Zhan, Q. Kuang, J. Z. Zhou, X. J. Kong, Z. X. Xie and L. S. Zheng, *J. Am. Chem. Soc.*, 2013, **135**, 1926–1933.
- M. Muller, X. Zhang, Y. Wang and R. A. Fischer, *Chem. Commun.*, 2009, 119–121.
- S. Hermes, F. Schröder, S. Amirjalayer, R. Schmid and R. A. Fischer, *J. Mater. Chem.*, 2006, **16**, 2464.
- (a) F. Ferey, C. Mellot-Draznieks, C. Serre, F. Millange, J. Dutour, S. Surble and I. Margiolaki, *Science*, 2005, **309**, 2040–2042; (b) A. Henschel, K. Gedrich, R. Kraehnert and S. Kaskel, *Chem. Commun.*, 2008, 4192–4194; (c) L. Bromberg, Y. Diao, H. Wu, S. A. Speakman and T. A. Hatton, *Chem. Mater.*, 2012, **24**, 1664–1675; (d) N. V. Maksimchuk, O. V. Zalomaeva, I. Y. Skobelev, K. A. Kovalenko, V. P. Fedin and O. A. Kholdeeva, *Proc. R. Soc. London, Ser. A*, 2012, **468**, 2017–2034.
- A. Modrow, D. Zargarani, R. Herges and N. Stock, *Dalton Trans.*, 2012, **41**, 8690–8696.
- X. Si, L. Sun, F. Xu, C. Jiao, F. Li, S. Liu, J. Zhang, L. Song, C. Jiang, S. Wang, Y. Liu and Y. Sawada, *Int. J. Hydrogen Energy*, 2011, **36**, 6698–6704.
- (a) H. Harada, T. Sakata and T. Ueda, *J. Am. Chem. Soc.*, 1985, **107**, 1773–1774; (b) X. Zong, G. Wu, H. Yan, G. Ma, J. Shi, F. Wen, L. Wang and C. Li, *J. Phys. Chem. C*, 2010, **114**, 1963–1968; (c) W. Zhang, Y. Wang, Z. Wang, Z. Zhong and R. Xu, *Chem. Commun.*, 2010, **46**, 7631–7633.
- (a) N. Bao, L. Shen, T. Takata and K. Domen, *Chem. Mater.*, 2007, **20**, 110–117; (b) M. Sathish, B. Viswanathan and R. Viswanath, *Int. J. Hydrogen Energy*, 2006, **31**, 891–898.
- (a) M. Alvaro, E. Carbonell, B. Ferrer, F. X. L. i Xamena and H. Garcia, *Chem.–Eur. J.*, 2007, **13**, 5106–5112; (b) B. Civalieri, F. Napoli, Y. Noël, C. Roetti and R. Dovesi, *CrystEngComm*, 2006, **8**, 364; (c) H. Li, M. Eddaoudi, M. O’Keeffe and O. M. Yaghi, *Nature*, 1999, **402**, 276–279.
- J. Juan-Alcañiz, J. Gascon and F. Kapteijn, *J. Mater. Chem.*, 2012, **22**, 10102.
- P. M. P. de Sousa, R. Grazina, A. D. S. Barbosa, B. de Castro, J. J. G. Moura, L. Cunha-Silva and S. S. Balula, *Electrochim. Acta*, 2013, **87**, 853–859.
- K. Sekizawa, K. Maeda, K. Domen, K. Koike and O. Ishitani, *J. Am. Chem. Soc.*, 2013, **135**, 4596–4599.
- X. Yong; and M. A. A. Schoonen, *Am. Mineral.*, 2000, **85**, 543–556.
- Y. Kataoka, K. Sato, Y. Miyazaki, K. Masuda, H. Tanaka, S. Naito and W. Mori, *Energy Environ. Sci.*, 2009, **2**, 397–400.